Inventory of Supplemental Information

A Novel Signal-Adaptor Interaction Mediates Sorting of the Alzheimer's Disease Amyloid Precursor Protein by the AP-4 Complex

Burgos, et al.

Supplemental Figures 1-5

Fig. S1, related to Fig. 2. Comparison of the crystal structures of the m4 and m2 C-terminal domain.

Fig. S2, related to Fig. 3. Interaction of APP peptide with binding site residues.

Fig. S3, related to Fig. 4.

(**A**) Comparison of the localizations of APP and AP-4 by immunofluorescence microscopy.

(**B**) Depletion of μ4 by RNAi.

(**C**) Disruption of YKFFE-μ4 interaction redistributes APP from endosomes to the TGN, and comparison of the turnover of APP in mock- and m4-depleted H4 neuroglioma cells.

(**D**) Transplantability of the YKFFE signal.

Fig. S4, related to Fig. 5.

(**A-B**) Disruption of the YKFFE-μ4 interaction does not affect acquisition of complex carbohydrates by APP.

(**C**) Disruption of YKFFE-μ4 interaction does not affect the expression levels of APP at the plasma membrane.

(**D**) Disruption of the YKFFE-μ4 interaction enhances g-secretase cleavage of the APP Swedish (Sw) mutant.

(**E-F**) Disruption of YKFFE-μ4 interaction enhances g-secretase cleavage of APP in H4 neuroglioma cells.

Fig. S5, related to Fig. 6. Disruption of the YKFFE-μ4 interaction enhances g-secretase cleavage of the APP Swedish (Sw) mutant in HeLa cells and of APP in H4 neuroglioma cells.

Supplemental Experimental Procedures

Supplemental References

A list of additional references used in the supplemental experimental procedures.

Supplemental Data

A Novel Signal-Adaptor Interaction Mediates Sorting of the Alzheimer's Disease Amyloid Precursor Protein by the AP-4 Complex

Patricia V. Burgos, Gonzalo A. Mardones, Adriana L. Rojas, Luis L. P. daSilva, Yogikala Prabhu, James H. Hurley and Juan S. Bonifacino

Supplemental Figures

Fig. S1

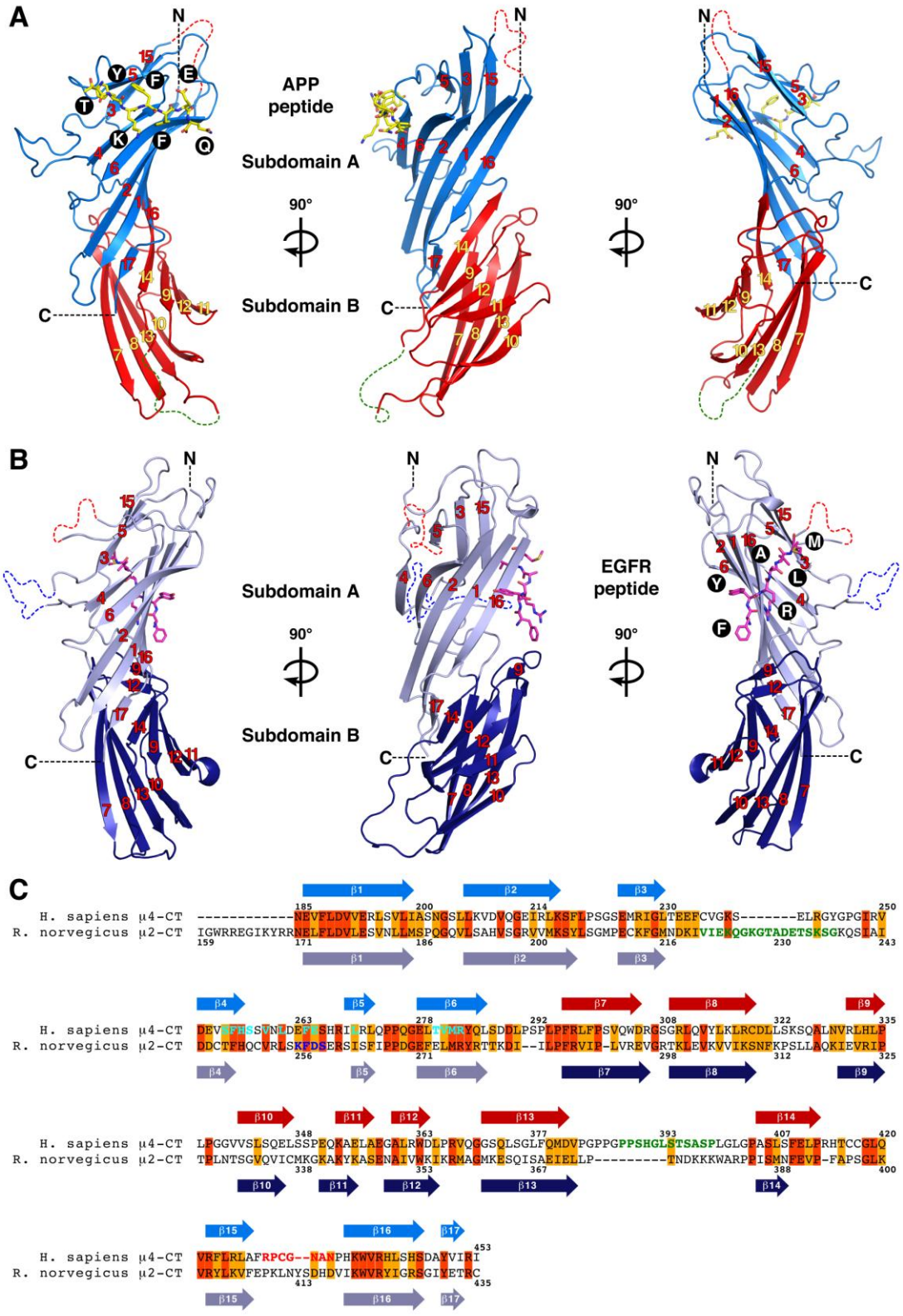

Fig. S2

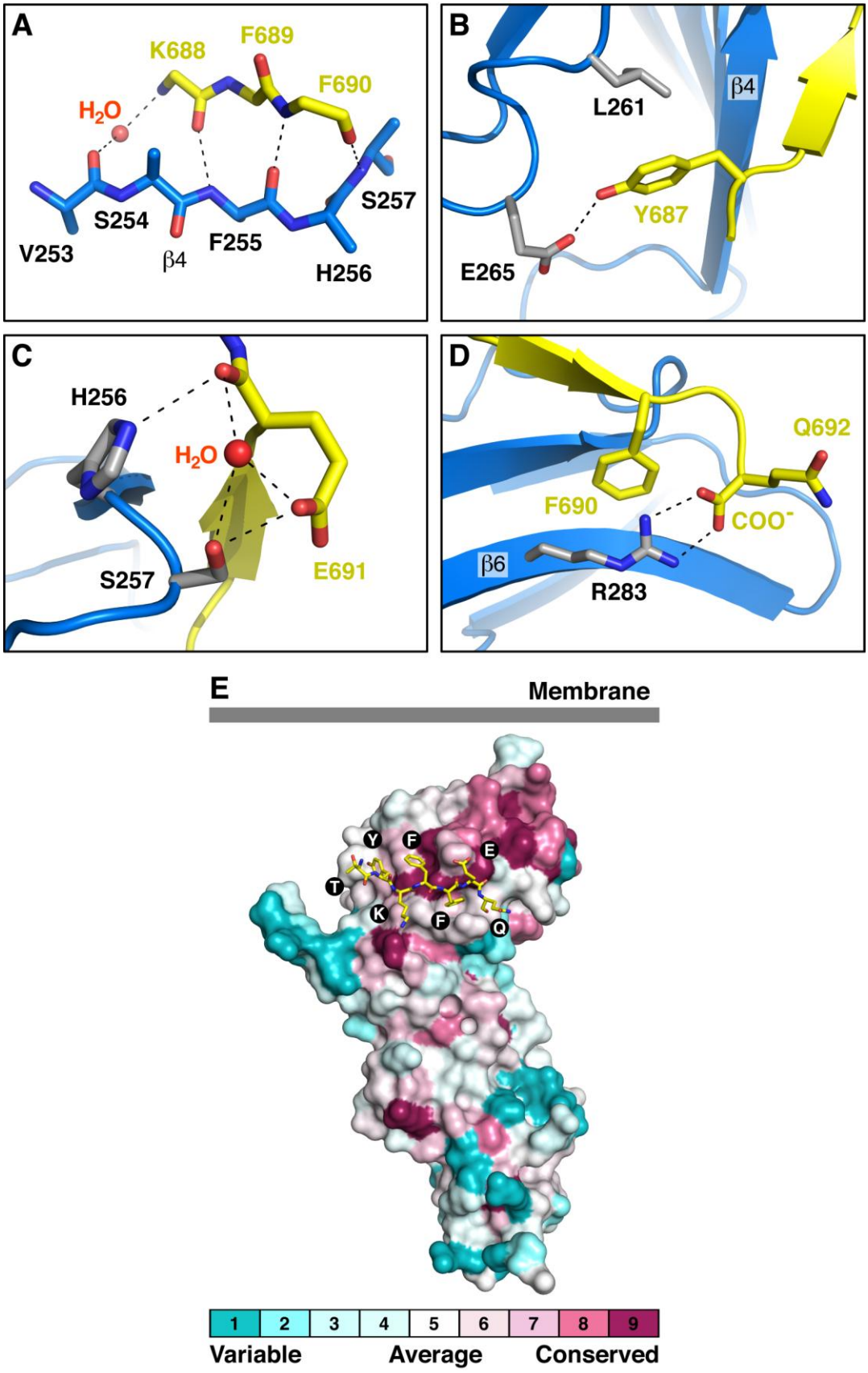
A
K688
F689
F690
H2O
S254
S257
V253
F255
β4
H256
B
L261
β4
Y687
E265
C
H256
H2O
S257
E691
D
Q692
F690
COO-
β6
R283
E
Membrane
Y
F
E
T
K
F
Q
1
2
3
4
5
6
7
8
9
Variable
Average
Conserved

Fig. S3

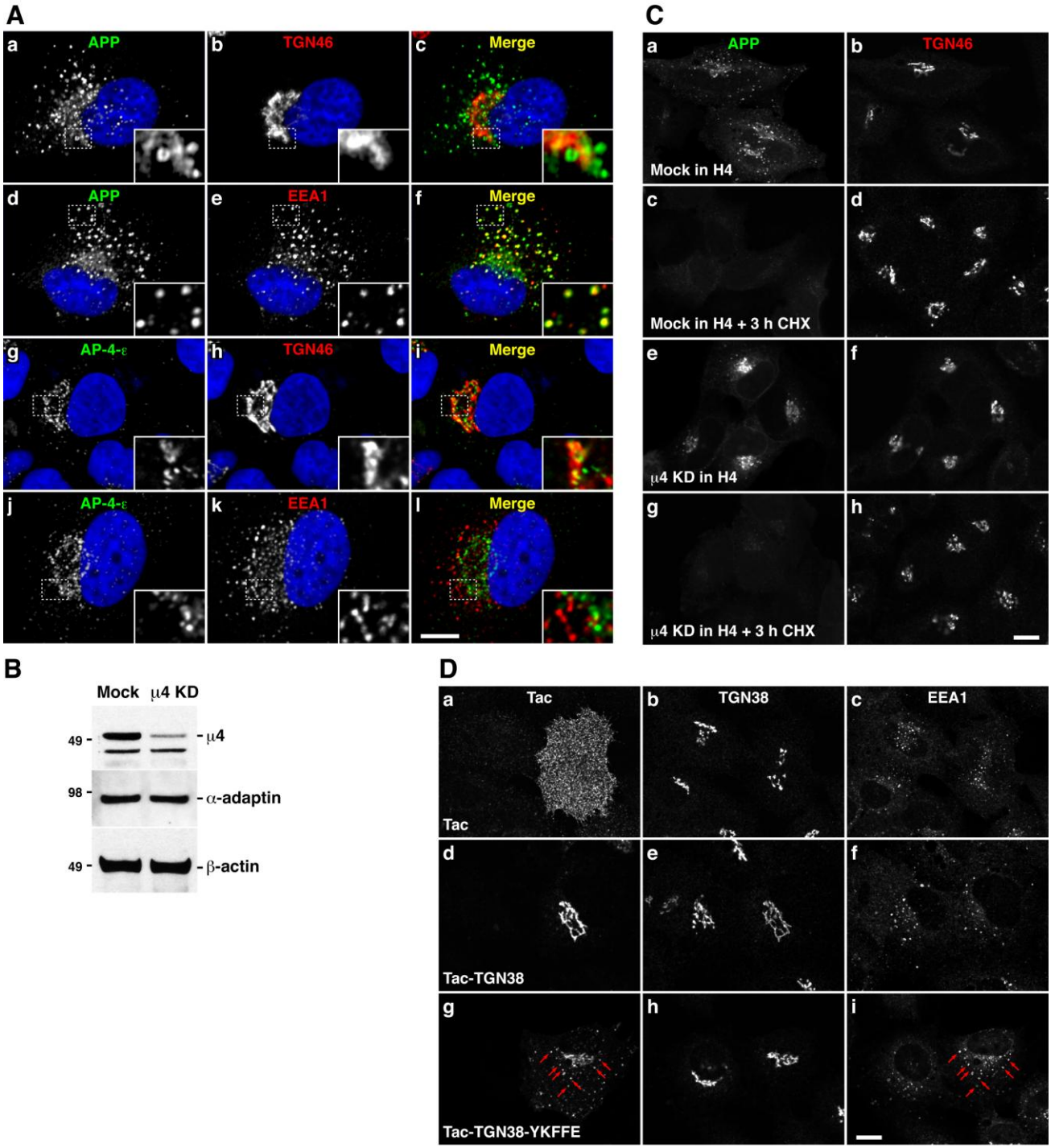
A
a APP
b TGN46
c Merge
d APP
e EEA1
f Merge
g AP-4-ε
h TGN46
i Merge
j AP-4-ε
k EEA1
l Merge
C
a APP
b TGN46
Mock in H4
c
d
Mock in H4 + 3 h CHX
e
f
μ4 KD in H4
g
h
μ4 KD in H4 + 3 h CHX
B
Mock
μ4 KD
49
μ4
98
α-adaptin
49
β-actin
D
a Tac
b TGN38
c EEA1
Tac
d
e
f
Tac-TGN38
g
h
i
Tac-TGN38-YKFFE

Fig. S4

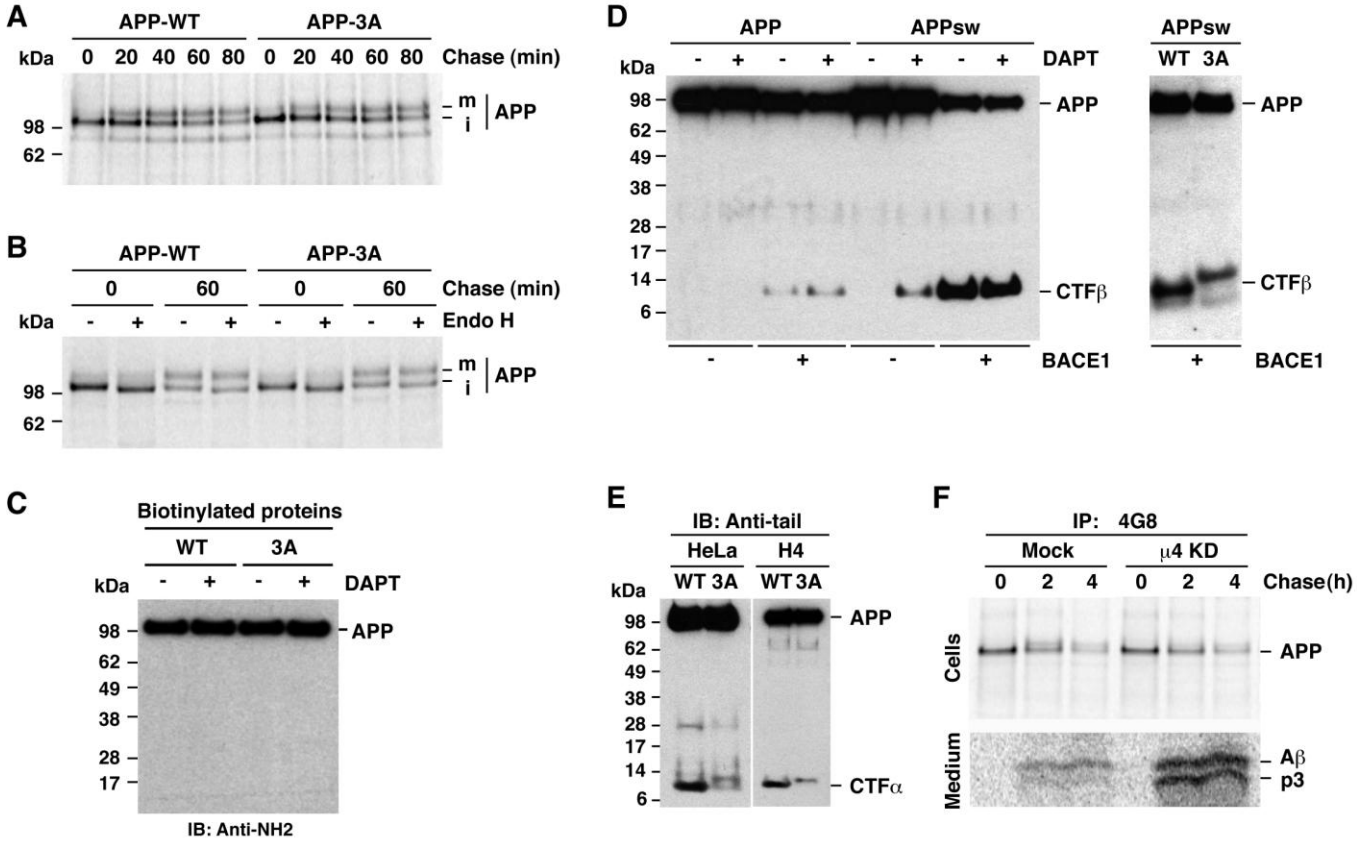
A
APP-WT
APP-3A
kDa
0 20 40 60 80 0 20 40 60 80
Chase (min)
98
62
m
i
APP
B
APP-WT
APP-3A
0
60
0
60
Chase (min)
kDa
- + - + - + - +
Endo H
98
62
m
i
APP
C
Biotinylated proteins
WT
3A
kDa
- + - +
DAPT
98
62
49
38
28
17
APP
IB: Anti-NH2
D
APP
APPsw
kDa
- + - + - + - +
DAPT
98
62
49
38
28
17
14
6
APP
CTFβ
- + - +
BACE1
APPsw
WT 3A
APP
CTFβ
+
BACE1
E
IB: Anti-tail
HeLa
H4
kDa
WT 3A WT 3A
98
62
49
38
28
17
14
6
APP
CTFα
F
IP: 4G8
Mock
μ4 KD
0 2 4 0 2 4
Chase(h)
Cells
APP
Medium
Aβ
p3

Fig. S5

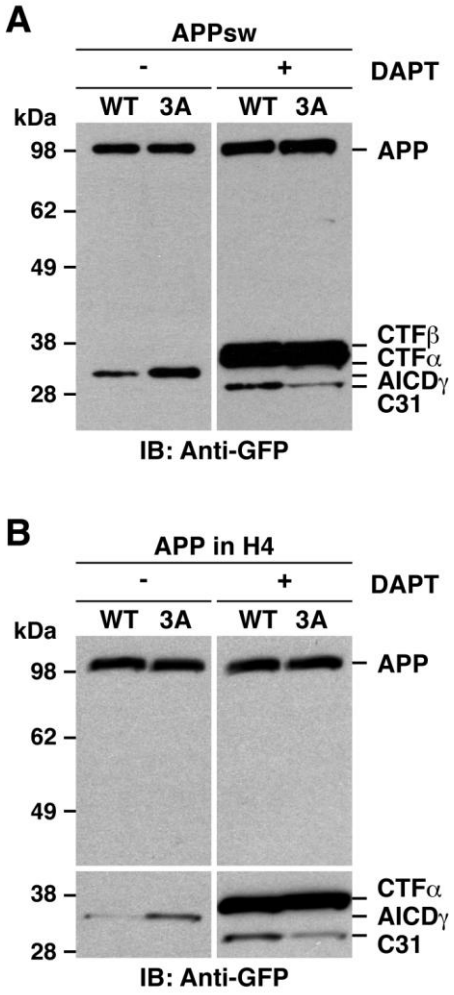
A
APPsw
-
+
DAPT
WT 3A WT 3A
kDa
98
62
49
38
28
APP
CTFβ
CTFα
AICDγ
C31
IB: Anti-GFP
B
APP in H4
-
+
DAPT
WT 3A WT 3A
kDa
98
62
49
38
28
APP
CTFα
AICDγ
C31
IB: Anti-GFP

Supplemental Figure Legends

Fig. S1, related to Fig. 2. Comparison of the crystal structures of the μ4 and μ2 C-terminal domain. (**A** and **B**) Cartoon views of human μ4 C-terminal domain with subdomain A in marine blue, subdomain B in red, and APP peptide (TYKFFEQ; stick model) in yellow, and of rat μ2 C-terminal domain (1BW8) with subdomain A in gray, subdomain B in dark blue (**A**), and EGFR peptide (FYRALM; stick model) in magenta (**B**). β sheet strands are numbered. The positions of the N- (N) and C-termini (C) are indicated. (**C**) Sequence alignment of the C-terminal domains of the solved structures of μ4 and μ2. Identical residues are shaded in red and conserved residues are shaded in orange. Disordered loops are in green (P388-P399) and red (P430-N435) letters in μ4 and in green (V221-G237) and blue (K256-S259) letters in μ2, and are represented in the respective colors as dashed lines in (**A**). The amino acids in the μ4 binding site (S254-R283) are in cyan letters. The β-strands in (**C**) (arrows) are colored as in (**A**).

Fig. S2, related to Fig. 3. Interaction of APP peptide with binding site residues. The stick representation of the TYKFFEQ peptide is shown with carbon atoms colored in yellow, and of the μ4 C-terminal domain with carbon atoms in marine blue (**A**) or gray (**B**-**D**). Hydrogen-bonds are indicated by dashed lines. (**A**) Direct and water-mediated β-sheet hydrogen bonding between the peptide and β4 strand of μ4. Side-chains are omitted for clarity. (**B**) The tyrosine in the peptide (Tyr-687) is in contact with Glu-265 and Leu-261 in μ4 via the hydroxyl group and the aromatic ring, respectively. (**C**) The main-chain carbonyl and side-chain carboxylate, respectively, of Glu-691 form hydrogen bonds with

His-256 and Ser-257. (**D**) Arg-283 forms a bidentate salt bridge with the C-terminal carboxylate of the peptide. The Arg-283 side-chain also makes a cation-π interaction with the aromatic ring of Phe-690. The numbers of the APP peptide residues are as in APP_{695}. (**E**) Conservation pattern for μ4 C-terminal domain determined with ConSurf. The μ4 C-terminal domain is presented as a surface model, and colored according to the conservation scores. The bar shows the coloring scheme. The peptide from the cytosolic tail of APP (TYKFFEQ) is shown in stick representation (carbon, yellow; oxygen, red; nitrogen, blue). The Bayesian method (Mayrose et al., 2004) was applied for the calculations of the conservation scores using the JTT matrix (Jones et al., 1992).

Fig. S3, related to Fig. 4. (**A**) Comparison of the localizations of APP and AP-4 by immunofluorescence microscopy. HeLa cells expressing HA-tagged APP were fixed, permeabilized, and double-labeled with rabbit antibody to the HA epitope (**a**, **d**), sheep antibody to TGN46 (**b**, **h**), mouse antibody to early endosome antigen-1 (EEA1) (**e**, **k**), and rabbit antibody to the ear domain (residues 849-1137) of AP-4-ε (**g**), followed by Alexa-488–conjugated donkey anti-rabbit IgG (green channel), Alexa-594–conjugated donkey anti-mouse IgG (red channel), or Alexa-647–conjugated donkey anti-sheep IgG (red channel). Nuclei were stained with Hoechst 33342 dye (blue channel). Merging red, green and blue channels generated the third picture on each row; yellow indicates overlapping localization of the green and red channels. Insets are 3X magnified images of the boxed areas. Bar: 10 μm. Notice the localization of APP to both the TGN and endosomes using the antibody to the luminal HA epitope. Staining of APP with an antibody to a cytosolic tail epitope resulted in more TGN staining (data not shown), probably due to the detection of both full-length APP and CTF products. (**B**) Depletion

of μ4 by RNAi. HeLa cells were transfected twice with siRNA directed to μ4 (μ4 KD) or mock-transfected (Mock). After lysis, the extracts were analyzed by SDS-PAGE and immunoblotting with a rabbit antibody to μ4, a rabbit antibody to α-adaptin subunit of AP-2, and a monoclonal antibody to β-actin as a loading control. The positions of molecular mass markers are indicated on the left. (**C**) Disruption of YKFFE-μ4 interaction redistributes APP from endosomes to the TGN, and comparison of the turnover of APP in mock- and μ4-depleted H4 neuroglioma cells. H4 cells were mock-transfected (**a-d**) or transfected twice with siRNA directed to μ4 (**e-h**), and re-transfected with a plasmid encoding APP-CFP. After 16 h cells were chased in the absence (**a-b**, **e-f**) or presence (**c-d**, **g-h**) of 100 μg/ ml cycloheximide for 3 h at 37°C. Cells were fixed, permeabilized, and labeled with sheep antibody to TGN46 and examined by confocal fluorescence microscopy as indicated above. Bar: 10 μm. (**D**) NRK cells were transfected with plasmids encoding either the Tac antigen (Tac) (**a-c**) or a chimeric protein consisting of Tac lumenal and transmembrane domains and the cytoplasmic domain of TGN38 (Tac-TGN38) (**d-f**) or chimeric Tac-TGN38 carrying the substitutions that replaced the YQRL for the YKFFE motif (Tac-TGN38-YKFFE) (**g-i**). Cells were stained for Tac, TGN38 and EEA1 and examined by confocal fluorescence microscopy. Arrows indicate foci of colocalization. Bar: 10 μm.

Fig. S4, related to Fig. 5. (**A-B**) Disruption of the YKFFE-μ4 interaction does not affect acquisition of complex carbohydrates by APP. HeLa cells transfected with either APP-CFP (WT) or APP-CFP with the triple mutation, F689A, F690A and E691A (3A), were pulse-labeled for 15 min with [^{35}S]methionine-cysteine and chased for 0-80 min at 37ºC. (**A**) APP species were immunoprecipitated from the cell lysates with polyclonal

antibody to GFP. Proteins were analyzed by SDS-PAGE and fluorography. (**B**) Immunoprecipitated APP species were treated with 60 U/ ml Endoglycosidase H (Endo H; New England Biolabs, Ipswich, MA) for 4 h at 37ºC and the proteins analyzed as indicated above. The positions of molecular mass markers are indicated on the left. Abbreviations: m, mature; i, immature. (**C**) Disruption of YKFFE-μ4 interaction does not affect the expression levels of APP at the plasma membrane. HeLa cells transfected with either HA-tagged APP (WT) or HA-tagged APP 3A mutant (3A) and incubated for 16h in the absence or presence of 250 nM DAPT were surface-labeled by biotinylation at 4ºC. After lysis, the extracts were incubated with Neutravidin-agarose and the bound proteins analyzed by immunoblotting (IB) with the indicated antibody to APP. The positions of molecular mass markers are indicated on the left. (**D**) Disruption of the YKFFE-μ4 interaction enhances γ-secretase cleavage of the APP Swedish (Sw) mutant. HeLa cells transfected with plasmids encoding either untagged APP (APP) or untagged APP bearing the Swedish double mutation K595N/ M596L (APPsw, WT), or untagged APPsw 3A mutant (F689A, F690A and E691A; 3A) were mock co-transfected (-) or co-transfected with a plasmid encoding β-secretase (BACE1) (+), and incubated in the absence (-) or presence (+) of 250 nM DAPT. Cell lysates were analyzed by SDS-PAGE and immunoblotting with the monoclonal antibody 6E10, which recognizes full-length APP and CTFβ, but not CTFα. (**E-F**) Disruption of YKFFE-μ4 interaction enhances γ-secretase cleavage of APP in H4 neuroglioma cells. (**E**) SDS-PAGE and immunoblot (IB) analysis with Anti-tail antibody of APP and CTF species from HeLa or H4 cells expressing APP-WT or APP-3A. (**F**) H4 cells transfected twice with siRNA directed to μ4 (μ4 knock-down or KD) or mock-transfected, and then re-transfected with a plasmid encoding HA-tagged APP, were pulse-labeled for 2 h at 37°C with 1 mCi/ ml

[^{35}S]methionine-cysteine and chased for 0-4 h at 37°C. After chase, APP species were immunoprecipitated from cell lysates or cell culture media with monoclonal antibody 4G8. Proteins were analyzed by SDS-PAGE and fluorography.

Fig. S5, related to Fig. 6. (**A-B**) Disruption of the YKFFE-μ4 interaction enhances γ-secretase cleavage of the APP Swedish (Sw) mutant in HeLa cells and of APP in H4 neuroglioma cells. HeLa cells expressing CFP-tagged APPsw (WT) or CFP-tagged APPsw 3A mutant (3A) (**A**), or H4 cells expressing APP-WT or APP-3A constructs tagged with CFP (**B**), were incubated in the absence (-) or presence (+) of 250 nM DAPT and analyzed by SDS-PAGE and immunoblotting with antibody to GFP. The positions of molecular mass markers and different APP species are indicated.

Supplemental Experimental Procedures

Recombinant DNAs, Site-directed Mutagenesis and Y2H Assays

The tail of APP (residues 649-695) and the last 18 C-terminal residues (676-695) were obtained by PCR amplification and cloned into TOPO 2.1 vector (Invitrogen, Carlsbad, CA). To generate Gal4bd-fusion constructs, these fragments were subcloned in-frame into the EcoRI and SalI sites of pGBKT7 (BD Biosciences Clontech, Palo Alto, CA). The cloning of all the other Y2H constructs has been described (Aguilar et al., 2001; Boehm et al., 2001). The μ1 and μ3 subunits used in Y2H experiments corresponded to the A isoforms. DNA fragments encoding either the Tac antigen or a chimeric DNA encoding the Tac lumenal and transmembrane domains and the cytoplasmic domain of TGN38

(Tac-TGN38), were obtained by PCR amplification from pCDM8-Tac and T-T-G plasmids, respectively (Humphrey et al., 1993), and cloned into the XhoI and KpnI sites of pEGFP-N1 (BD Biosciences Clontech, Mountain View, CA), including the stop-codon before the GFP coding sequence. The substitutions to introduce a YKFFE motif within the cytoplasmic tail of chimeric Tac-TGN38 (Tac-TGN38-YKFFE) were made using the QuikChange mutagenesis kit. The nucleotide sequences of all recombinant constructs were confirmed by dideoxy sequencing. The C-terminal CFP-tagged APP_{695} construct was provided by C. Dotti (Katholieke Universiteit Leuven, Belgium). The human BACE1 construct was provided by R. Doms (University of Pennsylvania, Philadelphia, PA). The CTFβ-GFP construct was provided by C. Haass (Ludwig-Maximilians Universität, München, Germany). Y2H assays were performed as previously described (Aguilar et al., 2001; Ohno et al., 1996; Ohno et al., 1995).

Expression and Purification of μ4 C-terminal domain constructs

Recombinant μ4 C-terminal domain constructs tagged with an N-terminal GST followed by a TEV protease cleavage site were expressed in *E. coli* B834(DE3)pLysS (Novagen, Madison, WI) after induction with 0.15 mM IPTG at 16°C for 48 h. Pellets were resuspended in 50 mM Tris-HCl (pH 8.0), 0.5 M NaCl, 5 mM β-mercaptoethanol, and protease inhibitors (Sigma), and lysed by sonication. The clarified supernatant was purified on glutathione-Sepharose 4B (GE Healthcare) and eluted with 20 mM reduced glutathione. N-terminal, His_6-tagged TEV protease was used to cleave the GST moiety. GST and TEV were removed by sequential passage through glutathione-Sepharose 4B and Ni-NTA resins (QIAGEN), and the μ4 C-terminal domain (μ4-C) was further

purified on a Superdex 200 column (GE Healthcare).

Isothermal Titration Calorimetry

Recombinant μ4-C constructs were dialyzed overnight at 4°C against excess ITC buffer (50 mM Tris-HCl, pH 7.4, 150 mM NaCl). APP peptides (ENPTYKFFEQ and ENPTAKAAEQ; New England Peptide, Gardner, MA) were also prepared in ITC buffer. All ITC experiments were carried out at 28°C using an iTC_{200} instrument (MicroCal LLC, Northampton, MA). Typically, the chamber contained 0.2 ml of 200-500 μM μ4-C constructs, and the APP peptides (2-5 mM) added in 16 injections of 2.45 μl each. Titration curves were analyzed using Origin software (MicroCal). The binding constant was calculated by fitting the curves corresponding to μ4-C to a one-site model.

Crystallization, Data collection and Structure Determination.

Unless otherwise stated, solutions and crystallization reagents were from Hampton Research (Aliso Viejo, CA). Crystals of the μ4 C-terminal domain in complex with the APP peptide ENPTYKFFEQ (New England Peptide) were grown by the hanging drop method at 21°C. The reservoir solution contained 0.1 M HEPES (pH 7.0), 15% (w/ v) PEG 6000 and 3% trimethylamine N-oxide dihydrate. Drops contained 1 μl reservoir solution and 3 μl of 10 mg/ ml protein-peptide complex. Prior to crystallization, the protein was incubated at room temperature for 1 h with 1.5 mM peptide. Under these conditions two crystal forms appeared in the same drops. Crystals were cryoprotected in the reservoir solution supplemented with 20% glycerol and then flash-cooled in liquid nitrogen. The first crystal form belonged to space group $P6_2/\ 6_4$ and diffracted to 3.3 Å resolution. The

second form belonged to space group $P2_1$ and diffracted to 1.6 Å resolution.

The structure was determined by the MAD method using the $P2_1$ crystal form. In order to increase the anomalous signal, a construct with an extra methionine (L424M) was engineered. Native $P2_1$ crystals were seeded into L424M SeMet drops. Crystals were grown by the hanging drop method at 21°C. The reservoir solution contained 0.1 M HEPES (pH 7.0), 10% (w/ v) PEG 3350 and 10 mM $MgCl_2$. Drops contained 2 μl of reservoir solution and 1 μl of 4.2 mg/ ml protein-peptide complex. Prior to crystallization, the protein was incubated at room temperature for 1 h with 240 μM peptide, and L424M SeMet crystals appeared after 18 h. A three-wavelength MAD data set was collected from the L424M SeMet crystal at the GM/ CA-CAT beamline 23-ID-D, and a native data set was collected at the SER-CAT beamline 22-ID-D at APS, Argonne National Laboratory. Diffraction images were processed and scaled with the program HKL2000 (Otwinowski and Minor, 1997). Data collection statistics for each data set are shown in Table 1. The positions of the 4 Se atoms were determined by Patterson search with the program SOLVE (Terwilliger and Berendzen, 1999). Subsequent phasing and solvent flattening was carried out using SOLVE and RESOLVE (Terwilliger, 2000) as implemented in PHENIX (Adams et al., 2002). A solvent-flattened MAD electron density synthesis was used for automatic construction of the μ4 C-terminal domain crystal structure with RESOLVE. The resulting model had a single chain of 232 residues correctly assigned among the 239 automatically built. Iterative manual model building and initial refinement were done using COOT (Emsley and Cowtan, 2004) and REFMAC. The final model was refined against the native dataset and has a single chain of 250 residues with 148 water molecules, 3 glycerol molecules and 7 residues from the APP cytosolic tail peptide.

Cell Culture, Transfection and RNAi

HeLa (human epithelial), and H4 (human neuroglioma) cells obtained from the American Type Culture Collection (Manassas, VA) were maintained in DMEM (Invitrogen) supplemented with 2 mM glutamine, 100 U/ ml penicillin, 100 μg/ ml streptomycin, and 10% (v/ v) fetal bovine serum (FBS; Invitrogen). For RNAi, cells were transfected twice at 72-h intervals with the siRNA using Oligofectamine (Invitrogen), and analyzed 72 h after the second round of transfection.

Other Antibodies

Horseradish peroxidase–conjugated donkey anti-mouse and donkey anti-rabbit IgG (GE Healthcare); Alexa-488– or -594–conjugated donkey anti-mouse IgG, Alexa-488– or -594–conjugated donkey anti-rabbit IgG, and Alexa-647–conjugated donkey anti-sheep IgG (Invitrogen).

Immunofluorescence Microscopy and Quantitative Analysis

Indirect immunofluorescence staining of fixed, permeabilized cells was performed as previously described (Mardones et al., 2007). Images were acquired with an Olympus FluoView FV1000 scanning unit fitted on an inverted Olympus IX81 microscope and equipped with a PlanApo 60x oil immersion objective (NA 1.40; Olympus, Melville, NY). For quantitative analysis 8-bit images were acquired under identical settings avoiding signal saturation, and corrected for noise, cross-talk, and background signals on each set of images. The percentage ± SD of Golgi localization of APP and T-T-G-

YKFFE constructs was calculated (n=15-20) from the integrated pixel intensity in the region of overlap with either TGN46 or TGN38.

Electrophoresis, Immunoblotting, Metabolic Labeling and Immunoprecipitation

SDS–PAGE, immunoblotting, immunoprecipitation and fluorography were performed as described (Mardones et al., 2007). For analysis of Aβ and p3 fragments, electrophoresis was performed on Novex 10-20% acrylamide Tricine gels (Invitrogen). Metabolic pulse-chase labeling was carried out with cells grown on six-well plates. The cells were pulse-labeled with either a short pulse of 15 min or a long pulse of 2-4 h at 37°C using 0.5-1 mCi/ ml [^{35}S]methionine-cysteine (Express Protein Label; Perkin Elmer-Cetus Life and Analytical Sciences, Boston, MA), and chased for 15 min to 4 h at 37°C in regular culture medium in the presence of 0.06 mg/ ml methionine and 0.1 mg/ ml cysteine. After chase, cells were rinsed twice with ice-cold PBS and subjected to lysis at 4°C in 50 mM Tris-HCl (pH 7.5), 150 mM NaCl, 5 mM EDTA, 1% (vol/ vol) Triton X-100, and a cocktail of protease inhibitors (Roche Applied Science). Antibodies were bound either to Protein-A- (for rabbit Anti-tail) or Protein-G- (for mouse monoclonal 4G8 and 6E10) Sepharose beads (GE Healthcare). Cell fractionation was conducted at 4°C. Cells grown on 6-well plates were scraped in 1 ml homogenization buffer containing 50 mM Tris-HCl (pH 7.4), 150 mM NaCl, 1 mM EDTA and 0.25 M sucrose and a cocktail of protease inhibitors (Roche Applied Science).

Cell Surface Biotinylation and Cell Fractionation

Cell surface biotinylation was conducted at 4°C. Cells were rinsed twice in PBS and exposed twice to 1 mM Sulfo-NHS-LC Biotin reagent (Pierce, Rockford, IL) in PBS for 30 min. The cells were subsequently washed, incubated in 50 mM NH_4Cl for 10 min to quench un-reacted ester, rinsed twice with PBS and lysed in 50 mM Tris-HCl, pH 7.5, 150 mM NaCl, 5 mM EDTA, 1% (vol/ vol) Triton X-100, and a cocktail of protease inhibitors (Roche Applied Science). Biotinylated proteins were isolated by sedimentation with Neutravidin-agarose (Pierce) in a rotary shaker for 2h at 4°C, washed and analyzed by SDS-PAGE and immunoblot with HRP–conjugated antibody to GFP. Cells were homogenized by 20 strokes in a 2-ml Dounce homogenizer and centrifuged at 800 *g* for 10 min to remove cell debris and nuclei. The supernatant was centrifuged at 100000 *g* for 20 min, and pellet and supernatant fractions were isolated and analyzed by SDS-PAGE and immunoblotting with HRP–conjugated antibody to GFP.

Supplemental References

Adams, P. D., Grosse-Kunstleve, R. W., Hung, L.-W., Ioerger, T. R., McCoy, A. J., Moriarty, N. W., Read, R. J., Sacchettini, J. C., Sauter, N. K., and Terwilliger, T.C. (2002). PHENIX: building new software for automated crystallographic structure determination. Acta Crystallogr D Biol Crystallogr *58*, 1948-1954.

Emsley, P., and Cowtan, K. (2004). Coot: model-building tools for molecular graphics. Acta Crystallogr D Biol Crystallogr *60*, 2126-2132.

Jones, D.T., Taylor, W.R. and Thornton, J.M. (1992). The rapid generation of mutation data matrices from protein sequences. Comput Appl Biosci, *8*, 275-282.

Mayrose, I., Graur, D., Ben-Tal, N. and Pupko, T. (2004). Comparison of site-specific rate-inference methods for protein sequences: empirical Bayesian methods are superior. Mol Biol Evol, *21*, 1781-1791.

Otwinowski, Z. and Minor, W. (1997). Processing of X-ray Diffraction Data Collected in Oscillation Mode. Methods Enzymol *276*, 307-326.

Terwilliger, T. C. (2000). Maximum-likelihood density modification. Acta Crystallogr D Biol Crystallogr *56*, 965-972.

Terwilliger, T. C. and Berendzen, J. (1999) Automated MAD and MIR structure solution. Acta Crystallogr D Biol Crystallogr *55*, 849-861.